

Finite-time H_∞ filtering for Markov jump systems with uniform quantization

Jingjing Dong(董敬敬), Xiaofeng Ma(马晓峰), Xiaoqing Zhang(张晓庆), Jianping Zhou (周建平), and Zhen Wang (王震)

Citation: Chin. Phys. B, 2023, 32 (**11**): 110202. DOI: 10.1088/1674-1056/acedf5
Journal homepage: http://cpb.iphy.ac.cn; http://iopscience.iop.org/cpb

What follows is a list of articles you may be interested in

An improved ISR-WV rumor propagation model based on multichannels with time delay and pulse vaccination

Yafang Dong(董雅芳), Liangán Huo(霍良安), Xiaoxiao Xie(谢笑笑), and Ming Li(李明)
Chin. Phys. B, 2023, 32 (**7**): 070205. DOI: 10.1088/1674-1056/acd2be

Rapid stabilization of stochastic quantum systems in a unified framework

Jie Wen(温杰), Fangmin Wang(王芳敏), Yuanhao Shi(史元浩), Jianfang Jia(贾建芳), and Jianchao Zeng(曾建潮)
Chin. Phys. B, 2023, 32 (**7**): 070203. DOI: 10.1088/1674-1056/acb9f3

Comparison of differential evolution, particle swarm optimization, quantum-behaved particle swarm optimization, and quantum evolutionary algorithm for preparation of quantum states

Xin Cheng(程鑫), Xiu-Juan Lu(鲁秀娟), Ya-Nan Liu(刘亚楠), and Sen Kuang(匡森)
Chin. Phys. B, 2023, 32 (**2**): 020202. DOI: 10.1088/1674-1056/ac65ee

Robustness measurement of scale-free networks based on motif entropy

Yun-Yun Yang(杨云云), Biao Feng(冯彪), Liao Zhang(张辽), Shu-Hong Xue(薛舒红), Xin-Lin Xie(谢新林), and Jian-Rong Wang(王建荣)
Chin. Phys. B, 2022, 31 (**8**): 080201. DOI: 10.1088/1674-1056/ac6942

Design of passive filters for time-delay neural networks with quantized output

Jing Han(韩静), Zhi Zhang(章枝), Xuefeng Zhang(张学锋), and Jianping Zhou(周建平)
Chin. Phys. B, 2020, 29 (**11**): 110201. DOI: 10.1088/1674-1056/aba602

Finite-time $\mathcal{H}_\infty$ filtering for Markov jump systems with uniform quantization

Jingjing Dong(董敬敬)[1], Xiaofeng Ma(马晓峰)[1], Xiaoqing Zhang(张晓庆)[1], Jianping Zhou(周建平)[1,†], and Zhen Wang(王震)[2]

[1] *School of Computer Science & Technology, Anhui University of Technology, Ma'anshan* 243032, *China.*
[2] *College of Mathematics & Systems Science, Shandong University of Science and Technology, Qingdao* 266590, *China*

(Received 31 May 2023; revised manuscript received 24 July 2023; accepted manuscript online 8 August 2023)

This paper is concerned with finite-time $\mathcal{H}_\infty$ filtering for Markov jump systems with uniform quantization. The objective is to design quantized mode-dependent filters to ensure that the filtering error system is not only mean-square finite-time bounded but also has a prescribed finite-time $\mathcal{H}_\infty$ performance. First, the case where the switching modes of the filter align with those of the MJS is considered. A numerically tractable filter design approach is proposed utilizing a mode-dependent Lyapunov function, Schur's complement, and Dynkin's formula. Then, the study is extended to a scenario where the switching modes of the filter can differ from those of the MJS. To address this situation, a mode-mismatched filter design approach is developed by leveraging a hidden Markov model to describe the asynchronous mode switching and the double expectation formula. Finally, a spring system model subject to a Markov chain is employed to validate the effectiveness of the quantized filter design approaches.

Keywords: Markov jump system, filter design, finite-time $\mathcal{H}_\infty$ performance, uniform quantization

PACS: 02.30.Yy, 02.50.Ga, 87.19.lr **DOI:** 10.1088/1674-1056/acedf5

1. Introduction

A Markov jump system (MJS) is a distinctive type of hybrid system comprising a collection of continuous-time (or discrete-time) subsystems, which are mathematically described by differential (or difference) equations, as well as a Markov process that governs the transitions occurring between these subsystems. MJSs are particularly useful for analyzing complex dynamic systems that are susceptible to unpredictable changes in parameters or structures caused by component or link failures.[1] The origins of theoretical research on these systems can be found in the 1960s. In 1961, Krasovskii and Lidskii[2] presented an initial model of MJSs and provided the corresponding control design scheme. Subsequently, Rishel[3] applied the dynamic programming method to discuss the optimal control problem of MJSs. Costa and do Val[4] further studied some fundamental issues of MJSs, including observability and measurability. In recent years, more topics related to MJSs, ranging from almost sure stability,[5] state estimation,[6] fault detection,[7] and dissipativity-based stabilization,[8] to sampled-data synchronization,[9] have been extensively investigated in the automation community.

Disturbances are often unavoidable in dynamic systems. Filtering, a specific type of state estimation, provides a means to estimate unmeasurable state variables while mitigating the impact of external disturbances. Broadly speaking, there are two categories of filtering methods: infinite-horizon filtering and finite-time filtering (FTF). The former focuses on the asymptotic stability of the filtering error system (FES) over an infinite time horizon, while the latter emphasizes the boundedness within a fixed time interval.[10] When faced with application scenarios where excessively large values arise during the state evolution, the FTF becomes a more suitable choice.[11] For MJSs, the investigation of FTF has emerged as an attractive research subject. In Ref. [12], Wu *et al*. explored a stochastic MJS and proposed an optimization-based FTF method. He *et al*.[13] established criteria to ensure the existence of finite-time $l_2 - l_\infty$ filters for discrete-time MJSs. In Ref. [14], Saravanan *et al*. examined the finite-time $\mathcal{H}_\infty$ filtering (FTHF) issue of delayed MJSs and presented a design methodology based on linear matrix inequalities (LMIs). It is noteworthy that the filter designs in these studies require the modes of the MJS and the filter to be fully matched, limiting their applicability to some degree.

The filtering strategies in the majority of existing studies are based on a traditional point-to-point architecture. With the rapid advancement of communication technology, signals between the sensor and the filter of a MJS can be transmitted through a wired or wireless network, forming a networked FES. The introduction of communication networks reduces wiring between the sensor and the filter, enabling data transmission across long distances. This results in cost savings and enhanced system flexibility.[15] Due to the limited communication bandwidth and network throughput, the measurement signals are often quantized to mitigate the communication load.[16] Two common types of quantization discussed in the literature on network-based filtering are logarithmic quantization and uniform quantization. In comparison to logarithmic quantization, uniform quantization, which utilizes fixed-point

†Corresponding author. E-mail: jpzhou0@gmail.com

© 2023 Chinese Physical Society and IOP Publishing Ltd

number representation, is considered easier to implement.[17] During the last few years, a number of attempts have been made on FTF for MJSs with logarithmic quantization.[18–20] However, to our knowledge, no research has been published on the FTF or FTHF for MJSs with uniform quantization effects.

Motivated by the above discussion, this paper revisits the FTHF issue for MJSs with signal quantization. The goal is to design quantized mode-dependent filters to ensure that the FES is not only mean-square finite-time bounded (MSFTB) but also has a prescribed finite-time $\mathcal{H}_\infty$ performance (FTHP) index. First, we consider the case where the switching modes of the filter align with those of the MJS. An LMIs-based filter design approach is put forward to achieve a predefined FTHP for the FES utilizing a mode-dependent Lyapunov function, Schur's complement, and Dynkin's formula. Then, we explore a more complex scenario where the switching modes of the filter are allowed to differ from those of the MJS. To address this, a mode-mismatched filter design method is developed by leveraging a hidden Markov model (HMM) to describe the asynchronous mode switching and the double expectation formula. Finally, we utilize a spring system model subject to a Markov chain to validate the quantized filter design approaches for the mode-matched and mode-mismatched cases, respectively.

The main contributions of this paper can be summarized as follows:

(i) Unlike previous studies on FTF for MJSs with signal quantization, the present work employs a uniform quantizer, designed as a piecewise function, to quantize the measurement output before transmission to the filter.

(ii) In contrast to the works of Refs. [12–14], which focused solely on the mode-matched filtering scenario, the present study encompasses both mode-matched and mode-mismatched filtering cases, and proposes the corresponding filter design approaches.

2. Preliminaries

In this section, we first describe the MJS model under consideration, explicitly formulate the FTHF issue, and then prepare some necessary lemmas. The notations involved throughout are standard unless explicitly stated otherwise.

2.1. Markov jump system model

We consider a continuous-time MJS described by

$$\begin{cases} \dot{\chi}(t) = A_{m_{\rm s}(t)}\chi(t) + D_{\chi m_{\rm s}(t)}\omega(t), \\ \xi(t) = C_{\xi m_{\rm s}(t)}\chi(t) + D_{\xi m_{\rm s}(t)}\omega(t), \\ \zeta(t) = C_{\zeta m_{\rm s}(t)}\chi(t) + D_{\zeta m_{\rm s}(t)}\omega(t), \end{cases} \tag{1}$$

where $\chi(t) \in \mathbb{R}^{n_\chi}$, $\xi(t) \in \mathbb{R}^{n_\xi}$, and $\zeta(t) \in \mathbb{R}^{n_\zeta}$ represent the system state, performance output signal to be estimated, and measurement output, respectively; $\omega(t) \in \mathbb{R}^{n_\omega}$ is the external disturbance, which, as in Refs. [21,22], satisfies

$$\int_0^{T_{\rm f}} \|\omega(t)\|^2 \,{\rm d}t \le d, \tag{2}$$

within which d is a given positive parameter and $[0, T_{\rm f}]$ is a fixed finite-time interval. In addition, $A_{m_{\rm s}(t)}$, $D_{\chi m_{\rm s}(t)}$, $C_{\xi m_{\rm s}(t)}$, $D_{\xi m_{\rm s}(t)}$, $C_{\zeta m_{\rm s}(t)}$, and $D_{\zeta m_{\rm s}(t)}$ represent the given parameter matrices subject to a Markov chain $\{m_{\rm s}(t)\}$ that takes values in set $\mathbb{S}_m = \{1, \ldots, m\}$ and is characterized by transition rate matrix $\Upsilon = (m_{{\rm s}r_1r_2})_{m\times m}$ with

$$\Pr\{m_{\rm s}(t+\Delta t) = r_2 \mid m_{\rm s}(t) = r_1\} = \begin{cases} 1 + m_{{\rm s}r_1r_2}\Delta t + o(\Delta t), & r_1 = r_2, \\ m_{{\rm s}r_1r_2}\Delta t + o(\Delta t), & r_1 \ne r_2, \end{cases} \tag{3}$$

where Δt is the infinitesimal transition time interval, implying that $\lim\limits_{\Delta t\to 0} \dfrac{o(\Delta t)}{\Delta t} = 0$. The variable $m_{{\rm s}r_1r_2}$ $(m_{{\rm s}r_1r_2} \ge 0, r_1 \ne r_2)$ denotes the transition rate from mode r_1 at moment t to mode r_2 at moment $t+\Delta t$ and satisfies[23,24]

$$m_{{\rm s}r_1r_1} = -\sum_{r_2=1, r_2\ne r_1}^{m} m_{{\rm s}r_1r_2}.$$

2.2. Uniform quantization

As shown in Fig. 1, the measurement output $\zeta(t)$ is quantized using a uniform quantizer before being transmitted to the filter to reduce the communication load. The quantizer $Q(\cdot)$ is defined as

$$Q(\zeta(t)) = \left[Q_1(\zeta_1(t)) \;\; Q_2(\zeta_2(t)) \;\; \cdots \;\; Q_{n_\zeta}(\zeta_{n_\zeta}(t))\right]^{\rm T},$$

where $Q_v(\zeta_v(t))$ $(v \in \{1, \ldots, n_\zeta\})$ are designed as the following piecewise function:

$$Q_v(\zeta_v(t)) = \begin{cases} \left\lfloor \dfrac{\zeta_v(t)}{\mathscr{E}_{\rm b}} + \dfrac{1}{2} \right\rfloor \mathscr{E}_{\rm b} & -\mathscr{T}_{\rm s} \le \zeta_v(t) < 0, 0 < \zeta_v(t) < \mathscr{T}_{\rm s}, \\ 0 & \zeta_v(t) = 0, \\ \mathscr{T}_{\rm s} - \dfrac{1}{2}\mathscr{E}_{\rm b} & \zeta_v(t) > \mathscr{T}_{\rm s}, \\ -\mathscr{T}_{\rm s} + \dfrac{1}{2}\mathscr{E}_{\rm b} & \zeta_v(t) < -\mathscr{T}_{\rm s}, \end{cases}$$

in which $\lfloor\cdot\rfloor$ is the round-down operation, and $\mathscr{E}_{\rm b}/2>0$ and $\mathscr{T}_{\rm s}>0$ represent the error bound and saturation threshold level, respectively. Clearly, for any $v\in\{1,\ldots,n_\zeta\}$, $Q_v(\zeta_v(t))$ satisfies the following properties

$$|Q_v(\zeta_v(t))-\zeta_v(t)|\leq\frac{1}{2}\mathscr{E}_{\rm b},\quad |\zeta_v(t)|\leq\mathscr{T}_{\rm s}, \tag{4}$$

$$|Q_v(\zeta_v(t))-\zeta_v(t)|>\frac{1}{2}\mathscr{E}_{\rm b},\ |\zeta_v(t)|>\mathscr{T}_{\rm s}. \tag{5}$$

Define $e_\zeta(t)=Q(\zeta(t))-\zeta(t)$. Then, from inequalities (4) and (5),

$$\left\|e_\zeta(t)\right\|\leq\frac{\sqrt{n_\zeta}}{2}\mathscr{E}_{\rm b} \tag{6}$$

holds when all quantizers $Q_1(\zeta_1(t)),\ldots,Q_{n_\zeta}(\zeta_{n_\zeta}(t))$ are not saturated.

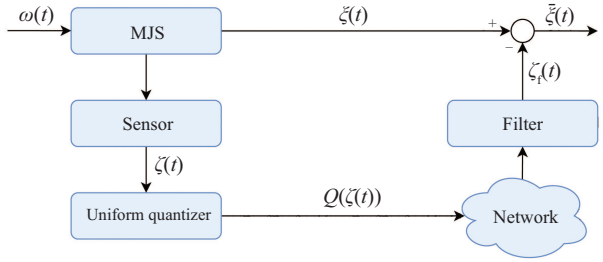


Fig. 1. The framework of filter design for MJS with uniform quantization.

2.3. Mode-dependent filter

The form of the mode-dependent filter is presented as follows:

$$\begin{cases}\dot{\chi}_{\rm f}(t)=A_{{\rm f}m_{\rm f}(t)}\chi(t)+B_{{\rm f}m_{\rm f}(t)}Q(\zeta(t)),\\ \xi_{\rm f}(t)=C_{{\rm f}m_{\rm f}(t)}\chi(t)+D_{{\rm f}m_{\rm f}(t)}Q(\zeta(t)),\end{cases} \tag{7}$$

where $\chi_{\rm f}(t)\in\mathbb{R}^{n_\chi}$ is the filter state, $\xi_{\rm f}(t)\in\mathbb{R}^{n_\xi}$ is the filter output signal, $\{m_{\rm f}(t)\}$ denotes the modes of the filter, and $A_{{\rm f}m_{\rm f}(t)}$, $B_{{\rm f}m_{\rm f}(t)}$, $C_{{\rm f}m_{\rm f}(t)}$, and $D_{{\rm f}m_{\rm f}(t)}$ represent the filter gains to be determined.

2.4. Filtering error system

Define $\bar{\chi}(t)=[\chi^{\rm T}(t)\quad\chi_{\rm f}^{\rm T}(t)]^{\rm T}$ and filtering error $\bar{\xi}(t)=\xi(t)-\xi_{\rm f}(t)$. Then combining MJS (1) with mode-dependent filter (7), we can derive an FES as follows:

$$\begin{cases}\dot{\bar{\chi}}(t)=\bar{A}_{m_{\rm s}(t)m_{\rm f}(t)}\bar{\chi}(t)+\bar{B}_{m_{\rm s}(t)m_{\rm f}(t)}\bar{\omega}(t),\\ \bar{\xi}(t)=\bar{C}_{m_{\rm s}(t)m_{\rm f}(t)}\bar{\chi}(t)+\bar{D}_{m_{\rm s}(t)m_{\rm f}(t)}\bar{\omega}(t),\end{cases} \tag{8}$$

where

$$\bar{A}_{m_{\rm s}(t)m_{\rm f}(t)}=\begin{bmatrix}A_{m_{\rm s}(t)} & 0\\ B_{{\rm f}m_{\rm f}(t)}C_{\zeta m_{\rm s}(t)} & A_{{\rm f}m_{\rm f}(t)}\end{bmatrix},$$

$$\bar{B}_{m_{\rm s}(t)m_{\rm f}(t)}=\begin{bmatrix}D_{\chi m_{\rm s}(t)} & 0\\ B_{{\rm f}m_{\rm f}(t)}D_{\zeta m_{\rm s}(t)} & B_{{\rm f}m_{\rm f}(t)}\end{bmatrix},$$

$$\bar{C}_{m_{\rm s}(t)m_{\rm f}(t)}=\begin{bmatrix}C_{\xi m_{\rm s}(t)}-D_{{\rm f}m_{\rm f}(t)}C_{\zeta m_{\rm s}(t)} & -C_{{\rm f}m_f(t)}\end{bmatrix},$$

$$\bar{D}_{m_{\rm s}(t)m_{\rm f}(t)}=\begin{bmatrix}D_{\xi m_{\rm s}(t)}-D_{{\rm f}m_f(t)}D_{\zeta m_{\rm s}(t)} & -D_{{\rm f}m_f(t)}\end{bmatrix},$$

$$\bar{\omega}(t)=\begin{bmatrix}\omega^{\rm T}(t) & e_\zeta{}^{\rm T}(t)\end{bmatrix}^{\rm T}.$$

We can further obtain from Eqs. (2) and (6) that

$$\int_0^{T_{\rm f}}\|\bar{\omega}(t)\|^2\,{\rm d}t=\int_0^{T_{\rm f}}\|\omega(t)\|^2\,{\rm d}t+\int_0^{T_{\rm f}}\left\|e_\zeta(t)\right\|^2{\rm d}t\leq\bar{d}, \tag{9}$$

where $\bar{d}=d+(n_\zeta/4)\mathscr{E}_{\rm b}^2T_{\rm f}$.

Remark 1 In contrast to prior studies on FTF for MJSs with signal quantization, the present work employs the uniform quantizer, designed as a piecewise function, to quantize the measurement output before transmitting it to the filter. However, this will result in the estimation of a time-independent upper bound for the quantization error, which poses challenges in handling. To tackle such an issue, inspired by Refs. [25,26], the quantization error is regarded as an additional disturbance term.

2.5. Problem statement

The definitions related to mean-square finite-time boundedness and FTHP are presented as follows.

Definition 1[27] Given scalars η_1, η_2, and $T_{\rm f}$ with $0<\eta_1<\eta_2$ and a matrix $H>0$, the FES is said to be MSFTB with regard to $(\eta_1,\eta_2,T_{\rm f},\bar{d},H)$ if

$$\mathbb{E}\left\{\bar{\chi}^{\rm T}(t)H\bar{\chi}(t)\right\}<\eta_2$$

holds under the condition that $\mathbb{E}\left\{\bar{\chi}^{\rm T}(0)H\bar{\chi}(0)\right\}\leq\eta_1$.

Definition 2[28] Given a scalar $\bar{\gamma}>0$, the FES is said to have the FTHP index $\bar{\gamma}$ if

$$\mathbb{E}\left\{\int_0^{T_{\rm f}}\left\|\bar{\xi}(t)\right\|^2{\rm d}t\right\}\leq\bar{\gamma}^2\mathbb{E}\left\{\int_0^{T_{\rm f}}\|\bar{\omega}(t)\|^2\,{\rm d}t\right\} \tag{10}$$

holds under the zero initial condition (i.e., $\bar{\chi}(0)=0$).

Now, the objective of this paper can be explicitly expressed as follows: to design a quantized mode-dependent filter (7) for MJS (1) such that the FES in Eq. (8) is not only MSFTB but also has a prescribed FTHP index $\bar{\gamma}$.

2.6. Necessary lemmas

To facilitate the establishment of the subsequent results, we introduce two lemmas.

Lemma 1[29] (Dynkin's formula) For any stopping times $0\leq t_0\leq t_1$, if $\mathcal{V}(\chi(t),m_{\rm s}(t))$ and $\mathcal{LV}(\chi(t),m_{\rm s}(t))$ are bounded on $t\in[t_0,t_1]$, then we have

$$\mathbb{E}\{\mathcal{V}(\chi(t_1),m_{\rm s}(t_1))\}=\mathbb{E}\{\mathcal{V}(\chi(t_0),m_{\rm s}(t_0))\}+\mathbb{E}\left\{\int_{t_0}^{t_1}\mathcal{LV}(\chi(t),m_{\rm s}(t))\,{\rm d}t\right\}.$$

Lemma 2[30] (Double expectation formula) For any random variables $\mathcal{M}$ and $\mathcal{N}$,

$$\mathbb{E}\{\mathcal{M}\} = \mathbb{E}\{\mathbb{E}\{\mathcal{M} \mid \mathcal{N}\}\}$$

holds, where $\mathbb{E}\{\mathcal{M} \mid \mathcal{N}\}$ is the conditional expectation given $\mathcal{N}$.

3. Mode-matched filter design

This section considers a simple mode-dependent filter referred to as the mode-matched filter, in which the switching modes of the filter are the same as those of MJS (1) (i.e., $m_{\mathrm{f}}(t) \equiv m_{\mathrm{s}}(t)$). The mode-matched filter is described as follows:

$$\begin{cases} \dot{\chi}_f(t) = A_{\mathrm{f}m_{\mathrm{s}}(t)}\chi(t) + B_{\mathrm{f}m_{\mathrm{s}}(t)}Q(\zeta(t)), \\ \xi_f(t) = C_{\mathrm{f}m_{\mathrm{s}}(t)}\chi(t) + D_{\mathrm{f}m_{\mathrm{s}}(t)}Q(\zeta(t)), \end{cases} \tag{11}$$

where $A_{\mathrm{f}m_{\mathrm{s}}(t)}$, $B_{\mathrm{f}m_{\mathrm{s}}(t)}$, $C_{\mathrm{f}m_{\mathrm{s}}(t)}$, and $D_{\mathrm{f}m_{\mathrm{s}}(t)}$ stand for filter gains to be determined. Combining mode-matched filter (11) with MJS (1), we can obtain the following FES

$$\begin{cases} \dot{\bar{\chi}}(t) = \bar{A}_{m_{\mathrm{s}}(t)}\bar{\chi}(t) + \bar{B}_{m_{\mathrm{s}}(t)}\bar{\omega}(t), \\ \bar{\xi}(t) = \bar{C}_{m_{\mathrm{s}}(t)}\bar{\chi}(t) + \bar{D}_{m_{\mathrm{s}}(t)}\bar{\omega}(t), \end{cases} \tag{12}$$

where

$$\begin{aligned} \bar{A}_{m_{\mathrm{s}}(t)} &= \begin{bmatrix} A_{m_{\mathrm{s}}(t)} & 0 \\ B_{fm_{\mathrm{s}}(t)}C_{\zeta m_{\mathrm{s}}(t)} & A_{\mathrm{f}m_{\mathrm{s}}(t)} \end{bmatrix}, \\ \bar{B}_{m_{\mathrm{s}}(t)} &= \begin{bmatrix} D_{\chi m_{\mathrm{s}}(t)} & 0 \\ B_{\mathrm{f}m_{\mathrm{s}}(t)}D_{\zeta m_{\mathrm{s}}(t)} & B_{\mathrm{f}m_{\mathrm{s}}(t)} \end{bmatrix}, \\ \bar{C}_{m_{\mathrm{s}}(t)} &= \begin{bmatrix} C_{\xi m_{\mathrm{s}}(t)} - D_{\mathrm{f}m_{\mathrm{s}}(t)}C_{\zeta m_{\mathrm{s}}(t)} & -C_{\mathrm{f}m_{\mathrm{s}}(t)} \end{bmatrix}, \\ \bar{D}_{m_{\mathrm{s}}(t)} &= \begin{bmatrix} D_{\xi m_{\mathrm{s}}(t)} - D_{\mathrm{f}m_{\mathrm{s}}(t)}D_{\zeta m_{\mathrm{s}}(t)} & -D_{\mathrm{f}m_{\mathrm{s}}(t)} \end{bmatrix}. \end{aligned}$$

A mode-matched filter design approach, which guarantees both mean-square finite-time boundedness and FTHP of FES (12), is provided in the following theorem.

Theorem 1 Given scalars $\gamma > 0$, $\alpha > 0$, β_1, and $\beta_2 > 0$, suppose that, for $r_1 \in \mathbb{S}_m$, there exist scalars $\rho_1 > 0$ and $\rho_2 > 0$ and matrices $P_{1r_1} > 0$ and $P_{2r_1} > 0$ such that the following LMIs hold:

$$\begin{bmatrix} \bar{P}_{r_1} + \mathscr{S}_{ym}\left(\Omega_{r_1}^{11}\right) - \alpha P_{r_1} & \Omega_{r_1}^{12} & \Omega_{r_1}^{13} \\ * & -\gamma^2 I & \Omega_{r_1}^{23} \\ * & * & -I \end{bmatrix} < 0, \tag{13}$$

$$\rho_1 H \le P_{r_1} \le \rho_2 H, \tag{14}$$

$$\eta_1\rho_2\,\mathrm{e}^{aT_{\mathrm{f}}} + \gamma^2\,\mathrm{e}^{aT_{\mathrm{f}}}\bar{d} < \eta_2\rho_1, \tag{15}$$

where

$$\begin{aligned} \bar{P}_{r_1} &= \sum_{r_2=1}^{m} m_{sr_1r_2}P_{r_2}, \\ P_{r_1} &= \begin{bmatrix} P_{1r_1} & \beta_1 P_{2r_1} \\ * & \beta_2 P_{2r_1} \end{bmatrix}, \\ \Omega_{r_1}^{11} &= \begin{bmatrix} P_{1r_1}A_{r_1} + \beta_1\bar{B}_{\mathrm{f}r_1}C_{\zeta r_1} & \beta_1\bar{A}_{fr_1} \\ \beta_1 P_{2r_1}A_{r_1} + \beta_2\bar{B}_{\mathrm{f}r_1}C_{\zeta r_1} & \beta_2\bar{A}_{\mathrm{f}r_1} \end{bmatrix}, \\ \Omega_{r_1}^{12} &= \begin{bmatrix} P_{1r_1}D_{\chi r_1} + \beta_1\bar{B}_{\mathrm{f}r_1}D_{\zeta r_1} & \beta_1\bar{B}_{\mathrm{f}r_1} \\ \beta_1 P_{2r_1}D_{\chi r_1} + \beta_2\bar{B}_{\mathrm{f}r_1}D_{\zeta r_1} & \beta_2\bar{B}_{\mathrm{f}r_1} \end{bmatrix}, \\ \Omega_{r_1}^{13} &= \begin{bmatrix} C_{\xi r_1} - \bar{D}_{\mathrm{f}r_1}C_{\zeta r_1} & -\bar{C}_{\mathrm{f}r_1} \end{bmatrix}^{\mathrm{T}}, \\ \Omega_{r_1}^{23} &= \begin{bmatrix} D_{\xi r_1} - \bar{D}_{\mathrm{f}r_1}D_{\zeta r_1} & -\bar{D}_{\mathrm{f}r_1} \end{bmatrix}^{\mathrm{T}}. \end{aligned}$$

Then, FES (12) is MSFTB with regard to $(\eta_1, \eta_2, T_{\mathrm{f}}, \bar{d}, H)$ and has the FTHP index $\bar{\gamma} = \gamma\sqrt{\mathrm{e}^{\alpha T_{\mathrm{f}}}}$ if the filter gains are chosen as

$$\begin{aligned} &A_{\mathrm{f}r_1} = P_{2r_1}^{-1}\bar{A}_{\mathrm{f}r_1}, \quad B_{\mathrm{f}r_1} = P_{2r_1}^{-1}\bar{B}_{\mathrm{f}r_1}, \\ &C_{\mathrm{f}r_1} = \bar{C}_{\mathrm{f}r_1}, \quad D_{\mathrm{f}r_1} = \bar{D}_{\mathrm{f}r_1}, \quad r_1 \in \mathbb{S}_m. \end{aligned} \tag{16}$$

Proof For $m_{\mathrm{s}}(t) = r_1 \in \mathbb{S}_m$, by applying Eqs. (12) and (16), we can rewrite inequality (13) as

$$\begin{bmatrix} \bar{P}_{r_1} + \mathscr{S}_{ym}(P_{r_1}\bar{A}_{r_1}) - \alpha P_{r_1} & P_{r_1}\bar{B}_{r_1} & \bar{C}_{r_1}^{\mathrm{T}} \\ * & -\gamma^2 I & \bar{D}_{r_1}^{\mathrm{T}} \\ * & * & -I \end{bmatrix} < 0. \tag{17}$$

By means of Schur's complement in Ref. [31], we deduce from inequality (17) that

$$\begin{bmatrix} \bar{P}_{r_1} + \mathscr{S}_{ym}(P_{r_1}\bar{A}_{r_1}) - \alpha P_{r_1} & P_{r_1}\bar{B}_{r_1} \\ * & -\gamma^2 I \end{bmatrix} + \begin{bmatrix} \bar{C}_{r_1}^{\mathrm{T}} \\ \bar{D}_{r_1}^{\mathrm{T}} \end{bmatrix}\begin{bmatrix} \bar{C}_{r_1} & \bar{D}_{r_1} \end{bmatrix} < 0. \tag{18}$$

Since

$$\begin{bmatrix} \bar{C}_{r_1}^{\mathrm{T}} \\ \bar{D}_{r_1}^{\mathrm{T}} \end{bmatrix}\begin{bmatrix} \bar{C}_{r_1} & \bar{D}_{r_1} \end{bmatrix} > 0,$$

we can derive from expression (18) that

$$\begin{bmatrix} \bar{P}_{r_1} + \mathscr{S}_{ym}(P_{r_1}\bar{A}_{r_1}) - \alpha P_{r_1} & P_{r_1}\bar{B}_{r_1} \\ * & -\gamma^2 I \end{bmatrix} < 0. \tag{19}$$

Consider the following mode-dependent Lyapunov function

$$\mathcal{V}(\bar{\chi}(t), m_{\mathrm{s}}(t)) = \bar{\chi}^{\mathrm{T}}(t)P_{m_{\mathrm{s}}(t)}\bar{\chi}(t). \tag{20}$$

Define $\mathcal{L}$ by the weak infinitesimal generator. Then, we have the following expression:

$$\mathcal{L}\mathcal{V}(\bar{\chi}(t), m_{\mathrm{s}}(t)) = \lim_{\Delta t \to 0}\frac{1}{\Delta t}\left(\mathbb{E}\{\mathcal{V}(\bar{\chi}(t+\Delta t), m_{\mathrm{s}}(t+\Delta t) \mid \bar{\chi}(t), m_{\mathrm{s}}(t))\} - \mathcal{V}(\bar{\chi}(t), m_{\mathrm{s}}(t))\right). \tag{21}$$

It follows from Eqs. (3), (20), and (21) that

$$\begin{aligned}
&\mathcal{L}\mathcal{V}(\bar{\chi}(t), m_{\rm s}(t)=r_1)\\
&=\lim_{\Delta t\to 0}\frac{1}{\Delta t}\left(\sum_{r_2=1}^{m}\Pr\{m_{\rm s}(t+\Delta t)=r_2\mid m_{\rm s}(t)=r_1\}\mathcal{V}(\bar{\chi}(t+\Delta t), m_{\rm s}(t+\Delta t)=r_2)-\bar{\chi}^{\rm T}(t)P_{r_1}\bar{\chi}(t)\right)\\
&=\lim_{\Delta t\to 0}\frac{1}{\Delta t}\left(\sum_{\substack{r_2=1\\ r_2\neq r_1}}^{m}(m_{{\rm s}r_1r_2}\Delta t+o(\Delta t))\,\bar{\chi}^{\rm T}(t+\Delta t)P_{r_2}\bar{\chi}(t+\Delta t)+(1+m_{{\rm s}r_1r_2}\Delta t+o(\Delta t))\,\bar{\chi}^{\rm T}(t+\Delta t)P_{r_1}\bar{\chi}(t+\Delta t)-\bar{\chi}^{\rm T}(t)P_{r_1}\bar{\chi}(t)\right)\\
&=\lim_{\Delta t\to 0}\frac{1}{\Delta t}\left(\sum_{r_2=1}^{m}(m_{{\rm s}r_1r_2}\Delta t+o(\Delta t))\,\bar{\chi}^{\rm T}(t+\Delta t)P_{r_2}\bar{\chi}(t+\Delta t)+\bar{\chi}^{\rm T}(t+\Delta t)P_{r_1}\bar{\chi}(t+\Delta t)-\bar{\chi}^{\rm T}(t)P_{r_1}\bar{\chi}(t)\right)\\
&=\bar{\chi}^{\rm T}(t)\bar{P}_{r_1}\bar{\chi}(t)+\dot{\mathcal{V}}(\bar{\chi}(t), m_{\rm s}(t)=r_1)\\
&=\bar{\chi}^{\rm T}(t)\bar{P}_{r_1}\bar{\chi}(t)+2\bar{\chi}^{\rm T}(t)P_{r_1}\dot{\bar{\chi}}(t).
\end{aligned}\tag{22}$$

This, together with FES (12), enables us to have that

$$\mathcal{L}\mathcal{V}(\bar{\chi}(t), m_{\rm s}(t)=r_1)=\bar{\chi}^{\rm T}(t)\bar{P}_{r_1}\bar{\chi}(t)+2\bar{\chi}^{\rm T}(t)P_{r_1}\bar{A}_{r_1}\bar{\chi}(t)+2\bar{\chi}^{\rm T}(t)P_{r_1}\bar{B}_{r_1}\bar{\omega}(t).\tag{23}$$

Based on Eqs. (20) and (23), we can write that

$$\begin{aligned}
&\mathbb{E}\left\{\mathcal{L}\mathcal{V}(\bar{\chi}(t), m_{\rm s}(t)=r_1)-\alpha\mathcal{V}(\bar{\chi}(t), m_{\rm s}(t)=r_1)-\gamma^2\|\bar{\omega}(t)\|^2\right\}\\
&=\mathbb{E}\left\{\bar{\chi}^{\rm T}(t)\bar{P}_{r_1}\bar{\chi}(t)+2\bar{\chi}^{\rm T}(t)P_{r_1}\bar{A}_{r_1}\bar{\chi}(t)+2\bar{\chi}^{\rm T}(t)P_{r_1}\bar{B}_{r_1}\bar{\omega}(t)-\alpha\bar{\chi}^{\rm T}(t)P_{r_1}\bar{\chi}(t)-\gamma^2\|\bar{\omega}(t)\|^2\right\}\\
&=\mathbb{E}\left\{\chi_\omega^{\rm T}(t)\begin{bmatrix}\bar{P}_{r_1}+\mathscr{S}_{ym}\left(P_{r_1}\bar{A}_{r_1}\right)-\alpha P_{r_1} & P_{r_1}\bar{B}_{r_1}\\ * & -\gamma^2 I\end{bmatrix}\chi_\omega(t)\right\},
\end{aligned}\tag{24}$$

where

$$\chi_\omega(t)=\left[\bar{\chi}^{\rm T}(t)\ \ \bar{\omega}^{\rm T}(t)\right]^{\rm T}.$$

We have from inequality (19) and Eq. (24) that

$$\mathbb{E}\left\{\mathcal{L}\mathcal{V}(\bar{\chi}(t), m_{\rm s}(t)=r_1)-\alpha\mathcal{V}(\bar{\chi}(t), m_{\rm s}(t)=r_1)-\gamma^2\|\bar{\omega}(t)\|^2\right\}<0.\tag{25}$$

Multiply both sides of inequality (25) by $\mathrm{e}^{-\alpha t}$, and we obtain

$$\mathbb{E}\left\{\mathcal{L}\left(\mathrm{e}^{-\alpha t}\mathcal{V}(\bar{\chi}(t), m_{\rm s}(t)=r_1)\right)-\gamma^2\mathrm{e}^{-\alpha t}\|\bar{\omega}(t)\|^2\right\}<0.$$

By using Dynkin's formula in Lemma 1, we can deduce that

$$\mathrm{e}^{-\alpha T_{\rm f}}\mathbb{E}\{\mathcal{V}(\bar{\chi}(t), m_{\rm s}(t)=r_1)\}-\mathbb{E}\{\mathcal{V}(0)\}<\gamma^2\int_0^{T_{\rm f}}\mathrm{e}^{-\alpha t}\|\bar{\omega}(t)\|^2\,\mathrm{d}t<\gamma^2\int_0^{T_{\rm f}}\|\bar{\omega}(t)\|^2\,\mathrm{d}t.\tag{26}$$

It follows from inequalities (9) and (26) that

$$\mathbb{E}\{\mathcal{V}(\bar{\chi}(t), m_{\rm s}(t)=r_1)\}<\mathrm{e}^{\alpha T_{\rm f}}\mathbb{E}\{\mathcal{V}(0)\}+\gamma^2\mathrm{e}^{\alpha T_{\rm f}}\bar{d}.\tag{27}$$

From Eq. (20) we have

$$\mathbb{E}\{\mathcal{V}(0)\}=\mathbb{E}\{\bar{\chi}^{\rm T}(0)P_{r_1}\bar{\chi}(0)\}=\mathbb{E}\left\{\bar{\chi}^{\rm T}(0)H^{1/2}\bar{H}_{Pr_1}H^{1/2}\bar{\chi}(0)\right\}\le\sup_{r_1\in\mathbb{S}_m}\{\lambda_{\max}(\bar{H}_{Pr_1})\}\mathbb{E}\{\bar{\chi}^{\rm T}(0)H\bar{\chi}(0)\},\tag{28}$$

$$\mathbb{E}\{\mathcal{V}(\bar{\chi}(t), m_{\rm s}(t)=r_1)\}=\mathbb{E}\left\{\bar{\chi}^{\rm T}(t)H^{1/2}\bar{H}_{Pr_1}H^{1/2}\bar{\chi}(t)\right\}\ge\inf_{r_1\in\mathbb{S}_m}\{\lambda_{\min}(\bar{H}_{Pr_1})\}\mathbb{E}\{\bar{\chi}^{\rm T}(t)H\bar{\chi}(t)\},\tag{29}$$

where $\bar{H}_{Pr_1}=H^{-1/2}P_{r_1}H^{-1/2}$. By substituting inequality (28) into inequality (27), we obtain

$$\mathbb{E}\{\mathcal{V}(\bar{\chi}(t), m_{\rm s}(t)=r_1)\}<\mathrm{e}^{\alpha T_{\rm f}}\left(\sup_{r_1\in\mathbb{S}_m}\{\lambda_{\max}(\bar{H}_{Pr_1})\}\mathbb{E}\{\bar{\chi}^{\rm T}(0)H\bar{\chi}(0)\}\right)+\gamma^2\mathrm{e}^{\alpha T_{\rm f}}\bar{d},$$

which, together with $\mathbb{E}\{\bar{\chi}^{\rm T}(0)H\bar{\chi}(0)\}\le\eta_1$, yields that

$$\mathbb{E}\{\mathcal{V}(\bar{\chi}(t), m_{\rm s}(t)=r_1)\}\le\mathrm{e}^{\alpha T_{\rm f}}\left(\sup_{r_1\in\mathbb{S}_m}\{\lambda_{\max}(\bar{H}_{Pr_1})\}\eta_1\right)+\gamma^2\mathrm{e}^{\alpha T_{\rm f}}\bar{d}.\tag{30}$$

Combining inequality (29) with inequality (30) results in

$$\mathbb{E}\left\{\bar{\chi}^{\mathrm{T}}(t)H\bar{\chi}(t)\right\} \leq \eta, \tag{31}$$

where

$$\eta = \frac{\eta_1 \sup_{r_1\in\mathbb{S}_m}\{\lambda_{\max}(\bar{H}_{Pr_1})\}\,\mathrm{e}^{\alpha T_{\mathrm{f}}} + \gamma^2\,\mathrm{e}^{\alpha T_{\mathrm{f}}}\bar{d}}{\inf_{r_1\in\mathbb{S}_m}\{\lambda_{\min}(\bar{H}_{Pr_1})\}}. \tag{32}$$

In addition, we deduce from inequality (14) that

$$\rho_1 I \leq \bar{H}_{Pr_1} \leq \rho_2 I,\ r_1 \in \mathbb{S}_m,$$

which implies that

$$\rho_1 \leq \inf_{r_1\in\mathbb{S}_m}\{\lambda_{\min}(\bar{H}_{Pr_1})\} \leq \sup_{r_1\in\mathbb{S}_m}\{\lambda_{\max}(\bar{H}_{Pr_1})\} \leq \rho_2. \tag{33}$$

According to inequality (15), expression (33) ensures that

$$\eta_1 \sup_{r_1\in\mathbb{S}_m}\{\lambda_{\max}(\bar{H}_{Pr_1})\}\,\mathrm{e}^{aT_{\mathrm{f}}} + \gamma^2\,\mathrm{e}^{aT_{\mathrm{f}}}\bar{d} < \eta_2 \inf_{r_1\in\mathbb{S}_m}\{\lambda_{\min}(\bar{H}_{Pr_1})\},$$

which, in conjunction with Eq. (32), enables us to get that

$$\eta < \eta_2. \tag{34}$$

From inequalities (31) and (34) we have

$$\mathbb{E}\left\{\bar{\chi}^{\mathrm{T}}(t)H\bar{\chi}(t)\right\} < \eta_2. \tag{35}$$

Thus, in view of Definition 1, FES (12) is MSFTB.

Finally, we show that FES (12) has the FTHP index $\bar{\gamma} = \gamma\sqrt{\mathrm{e}^{\alpha T_{\mathrm{f}}}}$. We obtain from Eqs. (12) and (24) that

$$\begin{aligned}&\mathbb{E}\left\{\mathcal{L}\mathcal{V}(\bar{\chi}(t),m_{\mathrm{s}}(t)=r_1) - \alpha\mathcal{V}(\bar{\chi}(t),m_{\mathrm{s}}(t)=r_1) - \gamma^2\|\bar{\omega}(t)\|^2 + \left\|\bar{\xi}(t)\right\|^2\right\}\\ &= \mathbb{E}\left\{\chi_{\omega}^{\mathrm{T}}(t)\begin{bmatrix}\bar{P}_{r_1} + \mathscr{S}_{ym}\left(P_{r_1}\bar{A}_{r_1}\right) - \alpha P_{r_1} + \bar{C}_{r_1}^{\mathrm{T}}\bar{C}_{r_1} & P_{r_1}\bar{B}_{r_1} + \bar{C}_{r_1}^{\mathrm{T}}\bar{D}_{r_1}\\ * & -\gamma^2 I + \bar{D}_{r_1}^{\mathrm{T}}\bar{D}_{r_1}\end{bmatrix}\chi_{\omega}(t)\right\},\end{aligned}$$

which, together with inequality (18), leads to

$$\mathbb{E}\left\{\mathcal{L}\mathcal{V}(\bar{\chi}(t),m_{\mathrm{s}}(t)=r_1) - \alpha\mathcal{V}(\bar{\chi}(t),m_{\mathrm{s}}(t)=r_1) - \gamma^2\|\bar{\omega}(t)\|^2 + \left\|\bar{\xi}(t)\right\|^2\right\} < 0. \tag{36}$$

By multiplying both side of inequality (36) by $\mathrm{e}^{-\alpha t}$ and then using Lemma 1, we can obtain

$$\mathbb{E}\{\mathcal{V}(T_{\mathrm{f}})\} < \mathrm{e}^{\alpha T_{\mathrm{f}}}\mathbb{E}\{\mathcal{V}(0)\} + \mathrm{e}^{\alpha T_{\mathrm{f}}}\mathbb{E}\left\{\int_0^{T_{\mathrm{f}}}\mathrm{e}^{-\alpha t}\left(\gamma^2\|\bar{\omega}(t)\|^2 - \left\|\bar{\xi}(t)\right\|^2\right)\mathrm{d}t\right\}. \tag{37}$$

Owing to that $\mathcal{V}(T_{\mathrm{f}}) > 0$ and $\mathcal{V}(0) = 0$, it follows from inequality (37) that

$$\mathbb{E}\left\{\int_0^{T_{\mathrm{f}}}\mathrm{e}^{-\alpha t}\left\|\bar{\xi}(t)\right\|^2 dt\right\} < \gamma^2\mathbb{E}\left\{\int_0^{T_{\mathrm{f}}}\mathrm{e}^{-\alpha t}\|\bar{\omega}(t)\|^2\,\mathrm{d}t\right\},$$

which, in conjunction with

$$\int_0^{T_{\mathrm{f}}}\mathrm{e}^{-\alpha t}\left\|\bar{\xi}(t)\right\|^2\mathrm{d}t > \mathrm{e}^{-\alpha T_{\mathrm{f}}}\int_0^{T_{\mathrm{f}}}\left\|\bar{\xi}(t)\right\|^2\mathrm{d}t, \quad \int_0^{T_{\mathrm{f}}}\mathrm{e}^{-\alpha t}\|\bar{\omega}(t)\|^2\,\mathrm{d}t < \int_0^{T_{\mathrm{f}}}\|\bar{\omega}(t)\|^2\,\mathrm{d}t$$

yields inequality (10). Thus, FES (12) has the FTHP index $\bar{\gamma}$ according to Definition 2. The proof is completed.

Remark 2 Theorem 1 presents a mode-matched filter design method by utilizing the mode-dependent Lyapunov function (20), Schur's complement, and Dynkin's formula. To eliminate the coupling terms, such as $P_{r_1}\bar{A}_{r_1}$, the Lyapunov matrix P_{r_1} is constructed as $\begin{bmatrix}P_{1r_1} & \beta_1 P_{2r_1}\\ * & \beta_2 P_{2r_1}\end{bmatrix}$. The introduction of two adjustable parameters β_1 and β_2 can significantly influence the FTHP.

4. Mode-mismatched filter design

In networked systems, it is common for the modes of the filter and system not to fully match due to network-induced constrains, such as data dropouts[32] and transmission delays.[33] Consequently, in this section we further explore the design of mode-mismatched filters. Specifically, the mode-mismatched filter model we consider is described by Eq. (7), where $\{m_{\mathrm{f}}(t)\}$ is another stochastic process correlated with the Markov process $\{m_{\mathrm{s}}(t)\}$, which is characterized by a conditional probability matrix (CPM) $\Lambda = (m_{\mathrm{f}r_1r_3})_{m\times n}$ with

$$m_{\mathrm{f}r_1r_3} = \Pr\left\{m_{\mathrm{f}}(t) = r_3 \mid m_{\mathrm{s}}(t) = r_1\right\},\ r_1 \in \mathbb{S}_m,\ r_3 \in \mathbb{S}_n,$$

where $\sum_{r_3=1}^{n} m_{\mathrm{f}r_1r_3} = 1$ and $\mathbb{S}_n = \{1,\ldots,n\}$.

Remark 3 The switching modes of filter are represented by the stochastic process $\{m_{\mathrm{f}}(t)\}$, which is distinct from the Markov process $\{m_{\mathrm{s}}(t)\}$ but hinges on it through the CPM. Motivated by Refs. [34–36], an HMM $(\{m_{\mathrm{s}}(t)\},\{m_{\mathrm{f}}(t)\},\Upsilon,\Lambda)$ is employed to characterize the mode-mismatched behavior between MJS (1) and filter (7). Note that when CPM Λ is an identity matrix, the switching modes of filter (7) align with those of MJS (1).

Theorem 2 Given scalars $\gamma>0$, $\alpha>0$, β_1, and $\beta_2>0$, suppose that, for $r_1\in\mathbb{S}_m$ and $r_3\in\mathbb{S}_n$, there exist scalars $\rho_1>0$ and $\rho_2>0$ and matrices $P_{1r_1}>0$, $P_2>0$, $R_{r_1r_3}$, and $G_{r_1r_3}$ such that LMIs (14), (15), and

$$\sum_{r_3=1}^{n} m_{fr_1r_3}R_{r_1r_3}\le 0, \tag{38}$$

$$\sum_{r_3=1}^{n} m_{\mathrm{f}r_1r_3}G_{r_1r_3}<\gamma^2 I, \tag{39}$$

$$\begin{bmatrix}\bar{P}_{r_1}+\mathscr{S}_{ym}\left(\Omega^{11}_{r_1r_3}\right)-\alpha P_{r_1}-R_{r_1r_3} & \Omega^{12}_{r_1r_3} & \Omega^{13}_{r_1r_3}\\ * & -G_{r_1r_3} & \Omega^{23}_{r_1r_3}\\ * & * & -I\end{bmatrix}<0 \tag{40}$$

hold, where

$$P_{r_1}=\begin{bmatrix}P_{1r_1} & \beta_1P_2\\ * & \beta_2P_2\end{bmatrix},$$

$$\Omega^{11}_{r_1r_3}=\begin{bmatrix}P_{1r_1}A_{r_1}+\beta_1\bar{B}_{\mathrm{f}r_3}C_{\zeta r_1} & \beta_1\bar{A}_{\mathrm{f}r_3}\\ \beta_1P_2A_{r_1}+\beta_2\bar{B}_{\mathrm{f}r_3}C_{\zeta r_1} & \beta_2\bar{A}_{\mathrm{f}r_3}\end{bmatrix},$$

$$\Omega^{12}_{r_1r_3}=\begin{bmatrix}P_{1r_1}D_{\chi r_1}+\beta_1\bar{B}_{\mathrm{f}r_3}D_{\zeta r_1} & \beta_1\bar{B}_{\mathrm{f}r_3}\\ \beta_1P_2D_{\chi r_1}+\beta_2\bar{B}_{\mathrm{f}r_3}D_{\zeta r_1} & \beta_2\bar{B}_{\mathrm{f}r_3}\end{bmatrix},$$

$$\Omega^{13}_{r_1r_3}=\begin{bmatrix}C_{\xi r_1}-\bar{D}_{\mathrm{f}r_3}C_{\zeta r_1} & -\bar{C}_{\mathrm{f}r_3}\end{bmatrix}^{\mathrm{T}},$$

$$\Omega^{23}_{r_1r_3}=\begin{bmatrix}D_{\xi r_1}-\bar{D}_{\mathrm{f}r_3}D_{\zeta r_1} & -\bar{D}_{\mathrm{f}r_3}\end{bmatrix}^{\mathrm{T}}.$$

Then, FES (8) is MSFTB with regard to $(\eta_1,\eta_2,T_{\mathrm{f}},\bar{d},H)$ and has the FTHP index $\bar{\gamma}=\gamma\sqrt{\mathrm{e}^{\alpha T_{\mathrm{f}}}}$ if the filtering gains are chosen as

$$A_{\mathrm{f}r_3}=P_2^{-1}\bar{A}_{\mathrm{f}r_3},\quad B_{\mathrm{f}r_3}=P_2^{-1}\bar{B}_{\mathrm{f}r_3},$$
$$C_{\mathrm{f}r_3}=\bar{C}_{\mathrm{f}r_3},\quad D_{\mathrm{f}r_3}=\bar{D}_{\mathrm{f}r_3},\quad r_3\in\mathbb{S}_n. \tag{41}$$

Proof For $m_{\mathrm{s}}(t)=r_1\in\mathbb{S}_m$ and $m_{\mathrm{f}}(t)=r_3\in\mathbb{S}_n$, using Eqs. (8) and (41), we can rewrite inequality (40) as follows:

$$\begin{bmatrix}\bar{P}_{r_1}+\mathscr{S}_{ym}\left(P_{r_1}\bar{A}_{r_1r_3}\right)-\alpha P_{r_1}-R_{r_1r_3} & P_{r_1}\bar{B}_{r_1r_3} & \bar{C}^{\mathrm{T}}_{r_1r_3}\\ * & -G_{r_1r_3} & \bar{D}^{\mathrm{T}}_{r_1r_3}\\ * & * & -I\end{bmatrix}<0.$$

Define $\Gamma_{r_1r_3}=\bar{P}_{r_1}+\mathscr{S}_{ym}\left(P_{r_1}\bar{A}_{r_1r_3}\right)-\alpha P_{r_1}+\bar{C}^{\mathrm{T}}_{r_1r_3}\bar{C}_{r_1r_3}$. Then, by utilizing Schur's complement in Ref. [31], it follows that

$$\begin{bmatrix}\Gamma_{r_1r_3}-R_{r_1r_3} & P_{r_1}\bar{B}_{r_1r_3}+\bar{C}^{\mathrm{T}}_{r_1r_3}\bar{D}_{r_1r_3}\\ * & -G_{r_1r_3}+\bar{D}^{\mathrm{T}}_{r_1r_3}\bar{D}_{r_1r_3}\end{bmatrix}<0, \tag{42}$$

which, in conjunction with $m_{\mathrm{f}r_1r_3}>0$ $(r_1\in\mathbb{S}_m, r_3\in\mathbb{S}_n)$, yields that

$$\sum_{r_3=1}^{n} m_{\mathrm{f}r_1r_3}\begin{bmatrix}\Gamma_{r_1r_3} & P_{r_1}\bar{B}_{r_1r_3}+\bar{C}^{\mathrm{T}}_{r_1r_3}\bar{D}_{r_1r_3}\\ * & -\gamma^2I+\bar{D}^{\mathrm{T}}_{r_1r_3}\bar{D}_{r_1r_3}\end{bmatrix}<\sum_{r_3=1}^{n} m_{\mathrm{f}r_1r_3}\begin{bmatrix}R_{r_1r_3} & 0\\ * & G_{r_1r_3}-\gamma^2I\end{bmatrix}. \tag{43}$$

Owing to the fact that

$$\sum_{r_3=1}^{n} m_{\mathrm{f}r_1r_3}\begin{bmatrix}\bar{C}^{\mathrm{T}}_{r_1r_3}\bar{C}_{r_1r_3} & \bar{C}^{\mathrm{T}}_{r_1r_3}\bar{D}_{r_1r_3}\\ * & \bar{D}^{\mathrm{T}}_{r_1r_3}\bar{D}_{r_1r_3}\end{bmatrix}=\sum_{r_3=1}^{n} m_{\mathrm{f}r_1r_3}\begin{bmatrix}\bar{C}^{\mathrm{T}}_{r_1r_3}\\ \bar{D}^{\mathrm{T}}_{r_1r_3}\end{bmatrix}\begin{bmatrix}\bar{C}_{r_1r_3} & \bar{D}_{r_1r_3}\end{bmatrix}>0,$$

we can derive from inequality (43) that

$$\sum_{r_3=1}^{n} m_{\mathrm{f}r_1r_3}\begin{bmatrix}\bar{P}_{r_1}+\mathscr{S}_{ym}\left(P_{r_1}\bar{A}_{r_1r_3}\right)-\alpha P_{r_1} & P_{r_1}\bar{B}_{r_1r_3}\\ * & -\gamma^2I\end{bmatrix}<\sum_{r_3=1}^{n} m_{\mathrm{f}r_1r_3}\begin{bmatrix}R_{r_1r_3} & 0\\ * & G_{r_1r_3}-\gamma^2I\end{bmatrix}. \tag{44}$$

Let us consider the Lyapunov function $\mathcal{V}(\bar{\chi}(t),m_{\mathrm{s}}(t))$ given in Eq. (20). From Eqs. (8) and (22), we have

$$\mathcal{L}\mathcal{V}(\bar{\chi}(t),m_{\mathrm{s}}(t)=r_1)=\bar{\chi}^{\mathrm{T}}(t)\bar{P}_{r_1}\bar{\chi}(t)+2\bar{\chi}^{\mathrm{T}}(t)P_{r_1}\bar{A}_{r_1m_{\mathrm{f}}(t)}\bar{\chi}(t)+2\bar{\chi}^{\mathrm{T}}(t)P_{r_1}B_{r_1m_{\mathrm{f}}(t)}\bar{\omega}(t). \tag{45}$$

Using Lemma 2, we get from Eqs. (20) and (45) that

$$\begin{aligned}&\mathbb{E}\left\{\mathcal{L}\mathcal{V}(\bar{\chi}(t),m_{\mathrm{s}}(t)=r_1)-\alpha\mathcal{V}(\bar{\chi}(t),m_{\mathrm{s}}(t)=r_1)-\gamma^2\|\bar{\omega}(t)\|^2\right\}\\
&=E\left\{\sum_{r_3=1}^{n}\Pr\{m_{\mathrm{f}}(t)=r_3\mid m_{\mathrm{s}}(t)=r_1\}\left(\bar{\chi}^{\mathrm{T}}(t)\bar{P}_{r_1}\bar{\chi}(t)+2\bar{\chi}^{\mathrm{T}}(t)P_{r_1}\bar{A}_{r_1r_3}\bar{\chi}(t)+2\bar{\chi}^{\mathrm{T}}(t)P_{r_1}B_{r_1r_3}\bar{\omega}(t)\right.\right.\\
&\left.\left.-\alpha\bar{\chi}^{\mathrm{T}}(t)P_{r_1}\bar{\chi}(t)-\gamma^2\|\bar{\omega}(t)\|^2\right)\right\}\\
&=\mathbb{E}\left\{\bar{\chi}^{\mathrm{T}}(t)\bar{P}_{r_1}\bar{\chi}(t)+2\bar{\chi}^{\mathrm{T}}(t)\sum_{r_3=1}^{n}m_{\mathrm{f}r_1r_3}P_{r_1}\bar{A}_{r_1r_3}\bar{\chi}(t)+2\bar{\chi}^{\mathrm{T}}(t)\sum_{r_3=1}^{n}m_{\mathrm{f}r_1r_3}P_{r_1}B_{r_1r_3}\bar{\omega}(t)-\alpha\bar{\chi}^{\mathrm{T}}(t)P_{r_1}\bar{\chi}(t)-\gamma^2\|\bar{\omega}(t)\|^2\right\}\\
&=\mathbb{E}\left\{\chi^{\mathrm{T}}_{\omega}(t)\sum_{r_3=1}^{n}m_{\mathrm{f}r_1r_3}\begin{bmatrix}\bar{P}_{r_1}+\mathscr{S}_{ym}\left(P_{r_1}\bar{A}_{r_1r_3}\right)-\alpha P_{r_1} & P_{r_1}\bar{B}_{r_1r_3}\\ * & -\gamma^2I\end{bmatrix}\chi_{\omega}(t)\right\},\end{aligned} \tag{46}$$

which, together with inequality (44), results in

$$\begin{aligned}
&\mathbb{E}\left\{\mathcal{L}\mathcal{V}(\bar{\chi}(t),m_{\rm s}(t)=r_1)-\alpha\mathcal{V}(\bar{\chi}(t),m_{\rm s}(t)=r_1)-\gamma^2\|\bar{\omega}(t)\|^2\right\}\\
&<\mathbb{E}\left\{\chi_{\omega}^{\rm T}(t)\sum_{r_3=1}^{n}m_{{\rm f}r_1r_3}\begin{bmatrix}R_{r_1r_3} & 0\\ * & G_{r_1r_3}-\gamma^2 I\end{bmatrix}\chi_{\omega}(t)\right\}\\
&=\mathbb{E}\left\{\bar{\chi}^{\rm T}(t)\sum_{r_3=1}^{n}m_{{\rm f}r_1r_3}R_{r_1r_3}\bar{x}(t)+\bar{\omega}^{\rm T}(t)\left(\sum_{r_3=1}^{n}m_{{\rm f}r_1r_3}G_{r_1r_3}-\gamma^2 I\right)\bar{\omega}(t)\right\}.
\end{aligned}\tag{47}$$

It follows from inequalities (38), (39), and (47) that

$$\mathbb{E}\left\{\mathcal{L}\mathcal{V}(\bar{\chi}(t),m_{\rm s}(t)=r_1)-\alpha\mathcal{V}(\bar{\chi}(t),m_{\rm s}(t)=r_1)-\gamma^2\|\bar{\omega}(t)\|^2\right\}<0,$$

which means FES (8) is MSFTB. The specific derivation process is identical to steps inequality (25) to Eq. (45) in Theorem 1 and we omitted here.

Next, we show that FES (8) has the FTHP index $\bar{\gamma}=\gamma\sqrt{{\rm e}^{\alpha T_{\rm f}}}$. For any $m_{\rm f}(t)=r_3\in\mathbb{S}_n$, we have from Eqs. (8) and (46) that

$$\begin{aligned}
&\mathbb{E}\left\{\mathcal{L}\mathcal{V}(\bar{\chi}(t),m_{\rm s}(t)=r_1)-\alpha\mathcal{V}(\bar{\chi}(t),m_{\rm s}(t)=r_1)-\gamma^2\|\bar{\omega}(t)\|^2+\left\|\bar{\xi}(t)\right\|^2\right\}\\
&=\mathbb{E}\left\{\chi_{\omega}^{\rm T}(t)\sum_{r_3=1}^{n}m_{{\rm f}r_1r_3}\begin{bmatrix}\Gamma_{r_1r_3} & P_{r_1}\bar{B}_{r_1r_3}+\bar{C}_{r_1r_3}^{\rm T}\bar{D}_{r_1r_3}\\ * & -\gamma^2 I+\bar{D}_{r_1r_3}^{T}\bar{D}_{r_1r_3}\end{bmatrix}\chi_{\omega}(t)\right\}.
\end{aligned}$$

From inequality (43), we get

$$\begin{aligned}
&\mathbb{E}\left\{\mathcal{L}\mathcal{V}(\bar{\chi}(t),m_{\rm s}(t)=r_1)-\alpha\mathcal{V}(\bar{\chi}(t),m_{\rm s}(t)=r_1)-\gamma^2\|\bar{\omega}(t)\|^2+\left\|\bar{\xi}(t)\right\|^2\right\}\\
&<\mathbb{E}\left\{\chi_{\omega}^{\rm T}(t)\sum_{r_3=1}^{n}m_{{\rm f}r_1r_3}\begin{bmatrix}R_{r_1r_3} & 0\\ * & G_{r_1r_3}-\gamma^2 I\end{bmatrix}\chi_{\omega}(t)\right\},
\end{aligned}$$

which, together with inequalities (38), (39), and (47), results in

$$\mathbb{E}\left\{\mathcal{L}\mathcal{V}(\bar{\chi}(t),m_{\rm s}(t)=r_1)-\alpha\mathcal{V}(\bar{\chi}(t),m_{\rm s}(t)=r_1)-\gamma^2\|\bar{\omega}(t)\|^2+\left\|\bar{\xi}(t)\right\|^2\right\}<0,$$

which means FES (8) has the FTHP index $\bar{\gamma}=\gamma\sqrt{{\rm e}^{\alpha T_{\rm f}}}$. The specific derivation process is identical to the proof of inequality (36) ensuring inequality (10) in Theorem 1 and we omitted here.

Remark 4 Theorem 2 further proposes a mode-mismatched filter design approach to ensure that FES (8) is MSFTB and has the FTHP index $\bar{\gamma}$. This design approach allows the switching modes of the filter to differ from those of the system while depending on it through conditional probabilities. To tackle the mode-mismatched filter design issue, as in Ref. [36], we introduce two decision variables $R_{r_1r_3}$ and $G_{r_1r_3}$ to separate inequality (40) from the conditional probability $m_{fr_1r_3}$. However, this may bring some conservatism, which will be verified in Section 5.

5. Example

In this section, we utilize the spring system model in Ref. [37] to illustrate the effectiveness of the proposed mode-matched and mode-mismatched filter design approaches. In Fig. 2, k_1 and k_2 denote the spring constants, and $M_{1m_{\rm s}(t)}$ and $M_{2m_{\rm s}(t)}$ represent the masses subject to a Markov chain $\{m_{\rm s}(t)\}$, which can take values 1 or 2.

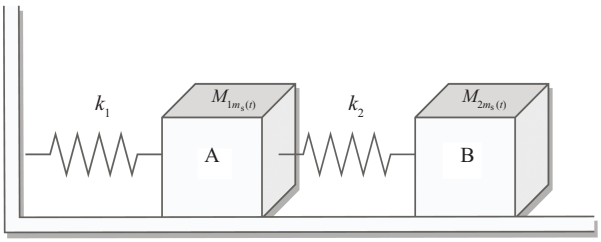


Fig. 2. Spring system model.

Furthermore, the coefficient of friction between objects A, B, and the horizontal surface is denoted by c. The spring system model can be described by Eq. (1), and its system matrices are given by

$$A_{m_{\rm s}(t)}=\begin{bmatrix}0 & 0 & 1 & 0\\ 0 & 0 & 0 & 1\\ -\dfrac{k_1+k_2}{M_{1m_{\rm s}(t)}} & \dfrac{k_2}{M_{1m_{\rm s}(t)}} & -\dfrac{c}{M_{1m_{\rm s}(t)}} & 0\\ \dfrac{k_2}{M_{2m_{\rm s}(t)}} & -\dfrac{k_2}{M_{2m_{\rm s}(t)}} & 0 & -\dfrac{c}{M_{2m_{\rm s}(t)}}\end{bmatrix},$$

$$D_{\chi m_s(t)} = \begin{bmatrix} 0 \\ 0 \\ \frac{1}{M_{1m_s(t)}} \\ 0 \end{bmatrix}, \quad C_{\zeta m_s(t)} = \begin{bmatrix} 1 & 0 & 0 & 0 \end{bmatrix},$$

$$C_{\xi m_s(t)} = \begin{bmatrix} 0 & 1 & 0 & 0 \end{bmatrix}, \quad D_{\zeta m_s(t)} = 0.2, D_{\xi m_s(t)} = 0.1,$$

$$k_1 = k_2 = 1, c = 2, M_{11} = 1, M_{12} = 2, M_{21} = 0.5, M_{22} = 1.$$

The uniform quantization and finite-time performance parameters are set as $\mathscr{T}_s = 10$, $\mathscr{E}_b = 0.05$, $\eta_1 = 1$, $\eta_2 = 36$, $d = 8$, $T_f = 20$, and $H = I$, respectively.

We first consider the mode-matched scenario. In this case, the existing literature on filtering under uniform quantization (see, *e.g.*, Refs. [38–40]) cannot be applied to find finite-time filters, while the design approaches proposed in Theorems 1 and 2 are applicable. In what follows, we take transition rate matrix as

$$\Upsilon = \begin{bmatrix} -0.5 & 0.5 \\ 0.8 & -0.8 \end{bmatrix}.$$

and set the CPM Λ to be an identity matrix. It should be noted that the smaller the FTHP index $\bar{\gamma}$, the better the performance of FES. Table 1 provides the minimum allowable FTHP index $\bar{\gamma}_{\min}$ for different values of β_1 and β_2 by solving the LMIs in Theorems 1 and 2, respectively. It can be observed from the table that adjusting the values of β_1 and β_2 can influence the minimum allowable FTHP index significantly. Furthermore, in comparison with the quantized filter design approach presented in Theorem 2, the one in Theorem 1 always achieves a better minimum allowable FTHP index $\bar{\gamma}_{\min}$. This outcome can be attributed to the introduction of additional variables $R_{r_1r_3}$ and $G_{r_1r_3}$ in Theorem 2, which induce extra conservatism.

Table 1. Minimum allowable FTHP index $\bar{\gamma}_{\min}$ for different values of β_1 and β_2.

$\bar{\gamma}_{\min}$	$\beta_1 = -0.05$ $\beta_2 = 0.06$	$\beta_1 = 0.95$ $\beta_2 = 1.06$	$\beta_1 = 1.95$ $\beta_2 = 2.06$	$\beta_1 = 2.95$ $\beta_2 = 3.06$	$\beta_1 = 3.95$ $\beta_2 = 4.06$
Theorem 1	0.9772	1.0745	1.2260	1.3240	1.3961
Theorem 2	0.9891	1.0949	1.2959	1.4708	1.6378

Next, we consider a mode-mismatched scenario where the CPM is set as

$$\Lambda = \begin{bmatrix} 0.6 & 0.4 \\ 0.5 & 0.5 \end{bmatrix}.$$

In this situation, the quantized filter design approach given in Theorem 1 is not applicable, while the approach presented in Theorem 2 can be utilized to ensure the mean-square finite-time boundedness and FTHP of the FES. In fact, if we set $\beta_1 = 1.5$ and $\beta_2 = 2$, then by using Theorem 2, we can obtain the minimum allowable FTHP index $\bar{\gamma}_{\min} = 0.9215$ and the corresponding filter gains as follows:

$$\left[\begin{array}{c|c} A_{f1} & B_{f1} \\ \hline C_{f1} & D_{f1} \end{array}\right] = \left[\begin{array}{cccc|c} -2.7107 & 0.8158 & -1.5656 & 4.7443 & -1.0821 \\ -0.1754 & -1.1932 & -1.8785 & -7.8291 & 0.1748 \\ -8.8622 & 3.3027 & -8.0927 & -5.3224 & -0.6693 \\ 0.4143 & 0.8245 & 2.6887 & -2.5117 & -0.0483 \\ \hline -0.0046 & -1.0217 & -0.0412 & 0.1477 & 0.1654 \end{array}\right],$$

$$\left[\begin{array}{c|c} A_{f2} & B_{f2} \\ \hline C_{f2} & D_{f2} \end{array}\right] = \left[\begin{array}{cccc|c} -1.3020 & 1.0051 & 3.9604 & -6.1533 & -1.1015 \\ 3.4234 & -3.9535 & -1.7319 & 12.5333 & 0.1789 \\ 7.1268 & -3.8618 & 4.9302 & 4.4487 & -0.6739 \\ 1.2077 & -2.5536 & -2.2811 & -1.0744 & -0.0303 \\ \hline -0.0171 & -1.0004 & -0.0453 & 0.1251 & 0.1614 \end{array}\right].$$

In this simulation, the external disturbance is given by

$$\omega(t) = 0.15\sin(t), \quad t \in [0, \infty),$$

and the initial values are set as $\chi(0) = [-0.4 \ -0.2 \ 0.4 \ 0.1]^T$ and $\chi_f(0) = [-0.5 \ -0.1 \ 0.3 \ 0.2]^T$.

Figures 3 and 4 show the switching modes of the Markov jump system and the filter, respectively, revealing the mode-mismatch behavior. Figure 5 shows the trajectories of the measurement output and the corresponding quantized measurement output. Figure 6 depicts the trajectory of $E\left\{\bar{\chi}^T(t)H\bar{\chi}(t)\right\}$. Clearly, throughout the time interval $[0, 20]$, the value of $E\left\{\bar{\chi}^T(t)H\bar{\chi}(t)\right\}$ consistently remains lower than $\eta_2 = 36$, which indicate that the FES is MSFTB. Lastly, we define the following equation

$$\gamma(t) = \sqrt{\frac{\mathbb{E}\left\{\int_0^t \left\|\bar{\xi}(s)\right\|^2 \mathrm{d}s\right\}}{\mathbb{E}\left\{\int_0^t \left\|\bar{\omega}(s)\right\|^2 \mathrm{d}s\right\}}}.$$

Then, figure 7 shows the trajectory of $\gamma(t)$ under the zero initial condition. We can find that the values of $\gamma(t)$ always stay below the minimum allowable FTHP index $\bar{\gamma}_{min} = 0.9215$. This shows the designed quantized mode-mismatched filter can ensure the FTHP of the FES.

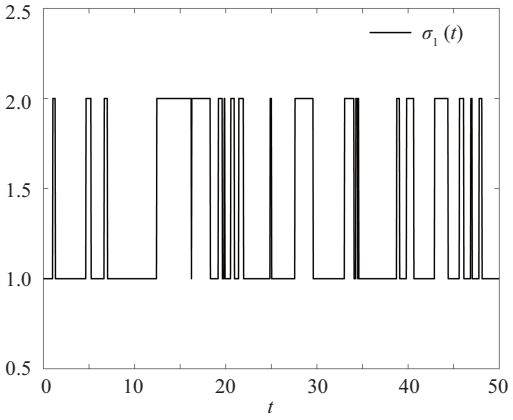


Fig. 3. Switching modes of the system.

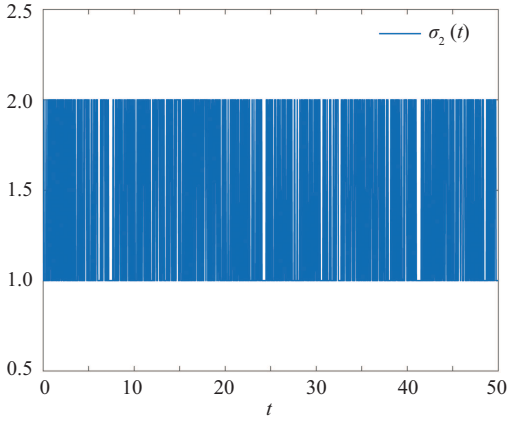


Fig. 4. Switching modes of filter.

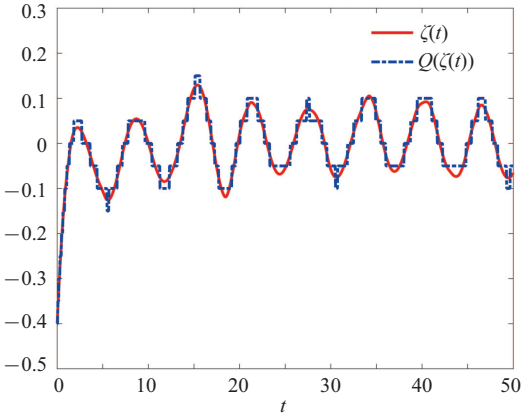


Fig. 5. Trajectories of $\zeta(t)$ and $Q(\zeta(t))$.

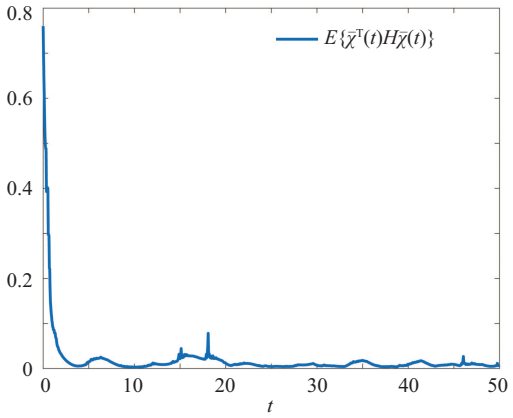


Fig. 6. Trajectory of $E\left\{\bar{\chi}^{\mathrm{T}}(t)H\bar{\chi}(t)\right\}$.

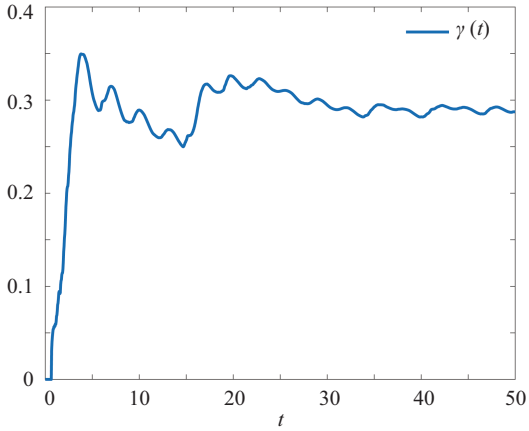


Fig. 7. Trajectory of $\gamma(t)$.

6. Conclusion

This work investigated the FTHF problem for MJSs with uniform quantization by considering two different mode-dependent filters. First, the case where the filter modes were the same as the system modes was considered. A mode-matched filter design method was given in Theorem 1 for MJS (1) to ensure that the FES is not only MSFTB but also satisfies a prescribed FTHP by employing a mode-dependent Lyapunov function, Schur's complement, and Dynkin's formula. Then, in order to solve the situation that the switching modes of the filter may differ from those of the MJS in practical systems, a mode-mismatched filter design approach was further proposed in Theorem 2 by leveraging an HMM to characterize the asynchronous mode switching between MJS (1) and filter (7) and the double expectation formula. Finally, a spring system model was utilized to validate the proposed filter design methods for the mode-matched and mode-mismatched cases, respectively.

Acknowledgement

Project supported by the Natural Science Foundation of the Anhui Higher Education Institutions (Grant Nos. KJ2020A0248 and 2022AH050310).

References

[1] Costa O L V, Fragoso M D and Todorov M G 2013 *Continuous-Time Markov Jump Linear Systems* (New York: Springer Science & Business Media)
[2] Krasovskii N N and Lidskii E A 1961 *Automat. Remote Control* **22** 1021
[3] Rishel R 1975 *SIAM J. Control* **13** 338
[4] Costa E F and do Val J B R 2001 *Syst. Control Lett.* **44** 135
[5] Li S Y and Lian J 2021 *IEEE Trans. Syst., Man, Cybern., Syst.* **51** 6681
[6] Shen H, Wu J C, Xia J W and Wang Z 2021 *Chin. Phys. B* **30** 060203
[7] Zhang X, Wang H, Stojanovic V, Cheng P, He S P, Luan X L and Liu F 2022 *IEEE Trans. Fuzzy Syst.* **30** 2487
[8] Tai W P, Li X L, Zhou J P and Arik S 2023 *Neural Netw.* **161** 55
[9] Yao L, Wang Z, Huang X, Li Y X, Ma Q and Shen H 2023 *IEEE Trans. Neural Netw. Learn. Syst.* **34** 909
[10] Amato F, Ariola M and Dorato P 2001 *Automatica* **37** 1459

[11] Song J S and Chang X H 2022 *IEEE Trans. Circuits Syst. II, Exp. Briefs* **69** 4369
[12] Wu Z T, Jiang B P and Kao Y G 2019 *IET Control Theory Appl.* **13** 702
[13] He Q G, Shi Z W, Wu D L, Fan S S, Zhang Z K and Liu D S 2022 *Int. J. Control, Autom. Syst.* **20** 2273
[14] Saravanan S, Syed Ali M, Alsulami H and Alhodaly M S 2020 *Int. J. Syst. Sci.* **51** 368
[15] Zhang L X, Gao H J and Kaynak O 2013 *IEEE Trans. Ind. Informat.* **9** 403
[16] Zhou J P, Dong J J and Xu S Y 2023 *IEEE Trans. Fuzzy Syst.* in press doi: 10.1109/TFUZZ.2023.3271348
[17] Mahmoud M S and Xia Y Q 2019 *Networked Control Systems: Cloud Control and Secure Control* (UK: Butterworth-Heinemann)
[18] Rathinasamy S, Murugesan S, Alzahrani F and Ren Y 2019 *Circuits, Syst. Signal Process.* **38** 3971
[19] Zhu Y C, Song X N, Wang M and Lu J W 2020 *Int. J. Control, Autom. Syst.* **18** 450
[20] Zhao Y, Wu B Y and Zhang W H 2023 *Int. J. Robust Nonlinear Control* in press doi: 10.1002/rnc.6704
[21] Sakthivel R, Kwon O M, Park M J and Sakthivel R 2023 *IEEE Trans. Syst., Man, Cybern., Syst.* **53** 3042
[22] Xiang Z R, Sun Y N and Mahmoud M S 2012 *Commun. Nonlinear. Sci. Numer. Simul.* **17** 1766
[23] Chen X, Yin L Y, Liu Y T and Liu H 2019 *Chin. Phys. B* **28** 090701
[24] Fang M, Shi P and Dong S L 2021 *IEEE Trans. Syst., Man, Cybern., Syst.* **51** 2916
[25] Sheng L, Wang Z D, Wang W B and Alsaadi F E 2017 *IEEE Trans. Syst., Man, Cybern., Syst.* **47** 1181
[26] Wang F, Wang Z D, Liang J L and Liu X H 2018 *IEEE Trans. Circuits Syst. I, Reg. Papers* **65** 2992
[27] Zhang X, He S P, Stojanovic V, Luan X L and Liu F 2021 *Sci. China Inf. Sci.* **64** 152206
[28] He S P and Liu F 2012 *IEEE Trans. Fuzzy Syst.* **20** 605
[29] Mao X R and Yuan C G 2006 *Stochastic Differential Equations with Markovian Switching* (London: Imperial College Press)
[30] Bickell P J and Doksum K A 2016 *Mathematical Statistics: Basic Ideas and Selected Topics, Volumes I-II Package* (USA: CRC Press)
[31] Boyd S, El Ghaoui L, Feron E and Balakrishnan V 1994 *Linear Matrix Inequalities in System and Control Theory* (Philadelphia, PA, USA:SIAM)
[32] Wu X R, Zhang Y C, Zhang T T and Zhang B L 2023 *Chin. Phys. B*, in press
[33] Duo L, Xiang L Y and Chen G R 2023 *Chin. Phys. B* **32** 060502
[34] Zhuang G M, Su S F, Xia J W and Sun W 2021 *IEEE Trans. Cybern.* **51** 1189
[35] Dong S L, Liu L, Feng G, Liu M Q, Wu Z G and Zheng R H 2022 *IEEE Trans. Cybern.* **52** 9882
[36] Qin X L, Dong J J, Zhou J P and Jiang T P 2023 *Commun. Nonlinear. Sci. Numer. Simul.* **121** 107242
[37] Gao H J and Chen T W 2007 *IEEE Trans. Autom. Control* **52** 2070
[38] Liu S, Wang Z D, Hu J and Wei G L 2020 *Int. J. Robust Nonlinear Control* **30** 7927
[39] Liu Y, Wang Z D, Liu C J, Coombes M and Chen W H 2023 *IEEE Trans. Ind. Informat.* **19** 5830
[40] Li M Y, Liang J L and Qiu J L 2023 *IEEE Trans. Circuits Syst. II, Exp. Briefs*, in press